Heat Treatment Effect on Erosion Characteristics of Hypereutectic Structured Hardface Overlay

Pardeep Kumar[1] and Buta Singh Sidhu[2]
[1]*Mechanical Engg. Section, Yadavindra College of Engineering, Punjabi University G.K. Campus, Talwandi Sabo, Distt. Bathinda, Punjab, India–151302*
[2]*Academics, Punjab Technical University, Jalandhar, Kapurthala Highway, Kapurthala, Punjab, India–144601*
E-mail: [1]pardeepjindal79@gmail.com

Abstract—*The solid particle erosion behaviour of a hardface overlay consisting of hypereutectic microstructure is studied. Erosion test parameters were chosen by simulating the conditions prevailing in pulverized coal burner nozzle (PCBN), used in thermal power plants to feed pulverized coal. The work was focused on to study the erosion behaviour of commercial hardfacing to prolong the service life of the PCBN. Hardfacing was performed with optimized welding parameters using manual metal arc welding. Erosion testing of the hardfaced test specimens, before and after heat treatment, was carried out in high temperature air-jet erosion test rig. Each specimen was tested for erosion at two different angles and three temperatures, freezing other test parameters. The hardface overlay was characterized with XRD analysis and SEM-EDS analysis. The influence of heat treatment on the micro-hardness and the microstructure was also studied to analyze their effect on erosion resistance. Refinement in microstructure was observed, leading to the change in erosion resistance of the overlay after heat treatment.*

Keywords*: Solid Particle Erosion, Hardfacing, Hypereutectic Microstructure, Pulverized Coal Burner Nozzle, Micro-hardness, Heat Treatment*

INTRODUCTION

It has been recognized since long that solid particle erosion (SPE) plays an important role in materials degradation [1–3]. ASTM defined SPE as the progressive loss of original material from a solid surface due to continued exposure to impacts by solid particles [4]. Wear mitigation is at the core of many resource-based industries, which rely heavily on wear resistant materials for extraction and processing, since equipment must endure particularly in aggressive conditions, which require abrasion, corrosion, and erosion resistance[5]. High temperature SPE is considered as the key material issue in the design and operation of thermal power plants and is recognized as one of the main causes of downtime in energy generation systems. Maintenance costs for replacing broken tubes in such installations have also been reported to be very high [6-8]. A wide range of components in thermal power generation systems like structural components of fluidized bed combustors, burner nozzles, pulverized fuel (PF) carrying bends and elbows, re-heater, super-heater, economiser tube banks, boiler heat exchanger, in bed tubes, tube banks, steam turbines, lock hopper valves, valve to throttle the flow of product stream etc. are exposed to erosive wear [9-15]. The rapid degradation of materials increases the overall cost of production, which marks it a multimillion-dollar problem [16, 7, 17-20]. The present work investigates the SPE behaviour of a commercial hardface overlay before and after heat treatment, when applied on SS 304, a material commonly used for the fabrication of pulverized coal burner nozzles (PCBNs). Pulverized coal is fed through the PCBN, which passes through it with a very high velocity and high mass flux. Both the factors makes the erosion problem more prominent leading to rapid degradation of the PCBNs. In this work, the erosion test conditions were simulated with the actual PCBN conditions, based upon the data collected from various thermal power plants of northern region of India. The properties of a material can be tailored by changing the microstructure through heat treatment. The SPE behaviour is reported to be linked with the microstructure however the microstructural features conductive for better erosion resistance are not available [21]. Limited investigations could be found through literature review regarding the SPE behaviour of hardfacings [13, 22, 23]. This work is an effort to study the effect of heat treatment and the obtained microstructure on SPE behaviour of a hardface overlay consisting two phase microstructure.

EXPERIMENTAL PROCEDURE

Materials and Hardfacing

Substrate steel SS 304 in 5 mm thick plate shape was hardfaced with a multi-carbide commercial electrode. The electrode was selected on the basis of its use in some of the thermal power plants of northern region of India for reclamation of eroded PCBNs. The nominal composition of the austenitic steel SS 304 is presented in Table [24]. The chemical composition of solid electrode wire was tested with optical emission spectroscopy (OES) and is presented in Table . Hardfacing was performed with metal arc welding using welding set-up of Larsen and Toubro make in the research lab at Yadavindra College of Engineering (YCoE), Talwandi Sabo. To remove moisture, the electrodes were dried in oven at a temperature of 100°C for 72 hours. The welding was performed at 126A and 19 volt AC current with a welding speed of 146 mm/min. Welding parameters were optimized using central composite design (CCD) technique of response surface methodology (RSM).

Important parameters of weld bead geometry (Fig.) namely bead width (W), penetration (P) and reinforcement (R) were considered as the output responses. Bead width and reinforcement were maximized, and penetration was minimized simultaneously using composite desirability optimization method [25].

Table 1: Nominal composition of SS 304

Element	Weight% [24]
Cr	18.0-20.0
Ni	8.0-10.5
Mn	2.00
Si	0.75
N	0.10
C	0.08
P	0.045
S	0.030
Fe	Balance

Table 2: Composition of Electrode, Tested with OES

Element	Weight %
Fe	42.86
Cr	35.51
C	9.65
Ni	5.11
Si	2.93
Mo	1.32
Nb	1.3
Ti	0.75
Mn	0.36

Weld beads were developed with 25% of overlapping in both the layers of weld overlay (see Fig. 1). Each weld layer was washed with acetone after cleaning with wire brush and chipping hammer. Top surface of the weld overlay was ground to remove the irregularities and small erosion test specimens were obtained after cutting with abrasive cut-off wheel. The heat treatment of the specimens was also done in order to study its effect on erosion behaviour. This was performed by heating the specimens to a temperature of 1050°C and then cooling after a soaking time of 1 hour. Hardfaced specimens (HF) were designated as HT after heat treatment. Specimens were flooded with coolant during cutting and grinding in order to protect grain structure. According to ASTM standard ASTM-G76-13 [26], the surface to be exposed to erodent attacks was polished down 1µm rms to obtain similar surface finish.

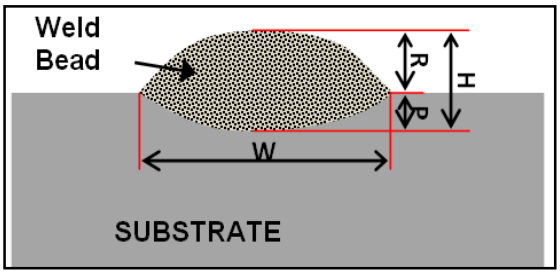

Fig. 1: Weld Bead Geometry

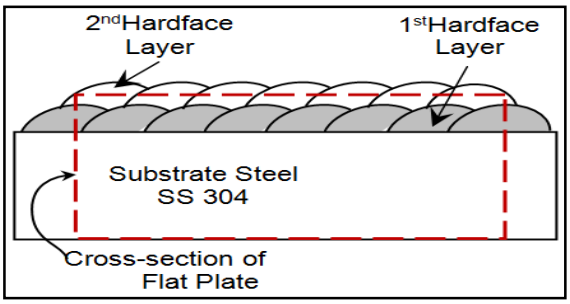

Fig. 2: Two Layer Weld Overlay Development and Grinding of Top Surface

Characterization

Hardfaced specimens before and after heat treatment were prepared for metallographic studies as per ASTM standard ASTM-E3-11 [27]. To reveal the grain boundaries, a mixture of 30% HCl, 30% HNO_3 and 40% water was used as etchant. Surface optical micrographs were captured at the inverted metallurgical microscope *(Radical Instruments make)* at Guru Kashi University, Talwandi Sabo. Thickness of hardface overlay was measured from the cross-sectional scanning electron microscope (SEM) images, according to ASTM standard ASTM-B487-85 [28]. Digital micro Vicker's hardness tester HM-211 *(Mitutoyo, Japan make)* was used for the measurement of micro-hardness, at the surface and cross-section, as per ASTM standard ASTM-E384-99 [29]. A load of 0.5 kgf was applied during testing and each reported value is the mean of five representative micro-indents. The chemical composition at different depths of the weld overlay was identified through cross-section field emission-scanning electron microscope/energy dispersive spectroscopy (FE-SEM/EDS) analysis on JSM-6610 (Jeol, New York make, with EDS attachment of Oxford, UK, installed with Genesis software) at IIT, Roorkee. FE-SEM/EDS analysis was aimed to understand the variation in chemical composition at different phases of the weld overlay and to get information about the extent of dilution. The X-ray diffraction (XRD) analysis from the surface of hardfaced specimen was carried out at IIT Ropar using XRD machine - PANalyticalX'Pert PRO MPD (Netherland) with Cu anode and K-α_1 K-α_2 radiations, having generator working at 40mA at a voltage of 45kV. The specimens were scanned in 2θ range of 10° to 110° and the intensities were recorded with goniometer radius of 240 mm set at PW3050/60 (θ/θ).

Erosion Testing

Erosion testing of the hardfaced specimens (with and without heat treatment) was carried out in high temperature air-jet erosion tester (TR-471-900, DUCOM make) at YCoE, Talwandi Sabo. Erosion testing was performed at two different angles and three different temperatures, freezing all other test parameters as

summarized in Table 3. The erosion test parameters were selected on the basis of conditions prevailing in the actual PCBN. Test specimens were bombarded with air carrying angular alumina particles having average particle size of 50μm. Each tested specimen was weighed in digital electronic weighing balance *(Citizen make, accuracy 0.1 mg)* before and after the test, to record the weight loss during erosion testing. In order to observe any weight change due to oxidation in high temperature testing, an additional specimen was kept in the test rig. This additional specimen was positioned away from the erodent attacks but remained exposed to similar environmental conditions. The weight change data of the additional specimen was also recorded.

Table 3: Erosion Test Conditions

Nozzle Material	Alumina
Nozzle inner diameter	3 ± 0.075 mm
Nozzle length	75 mm
Stand-off distance	10±1 mm
Air pressure	2 bar
Velocity	51.15 m/sec.
Erodent flux	10.25 kg/m^{2}sec.
Temperatures	Room temperature, 200°C, 400°C
Angles of impingement	30°, 90°
Test duration	1 hour

RESULTS AND DISCUSSION

Characterization

The thickness of finished erosion test specimen, as measured from cross-sectional BSEI (see Fig. 3) was obtained to be 1511 μm. The average value of thickness measured at five distinct points is reported. However the thickness of as-hardfaced specimens was reduced due to grinding performed for obtaining smooth and similar surface finish.

SEM-EDS Analysis

The variation in chemical composition at different points in the base and overlay region is presented in Fig. 3 along with the SEM micrograph. The chemical composition seems to be identical with the results of spectroscopy (Table 2). The variation in elemental composition along the cross-section may be due the distribution of phases of different metal carbides. Throughout the cross-section, large proportions of iron consistent with the elemental compositions of the base and that of the electrode were observed. Relatively higher proportion of chromium was observed in the overlay region and carbon percentage was more than 10% indicating the formation chromium carbides. Nickel was also observed in the overlay region but the proportion is less as compared to that in the substrate. Manganese and silicon were also observed in very small proportions.

XRD Analysis

Phase composition analysis obtained through XRD is presented in Fig. 4. Multiple metal carbides of type M_7C_3 containing mainly Fe and Cr can be seen in XRD profiles. Major peaks of $(Cr, Fe)_7C_3$, Cr_7C_3, Fe_7C_3 and Mn_7C_3 are seen. Cementite (Fe_3C) and chromium carbide (Cr_3C_2) are observed in minor phase. Chromium and iron rich carbides, as discerned in the major phases of X-ray diffractogram also confirm the results of OES (Table 2) and SEM-EDS analysis (Fig. 3).

Metallographic Studies

Surface microstructure of hard face overlay (HF) as presented in Fig. 5(a) is a typical hypereutectic microstructure. Hexagonal shaped coarse metal carbides

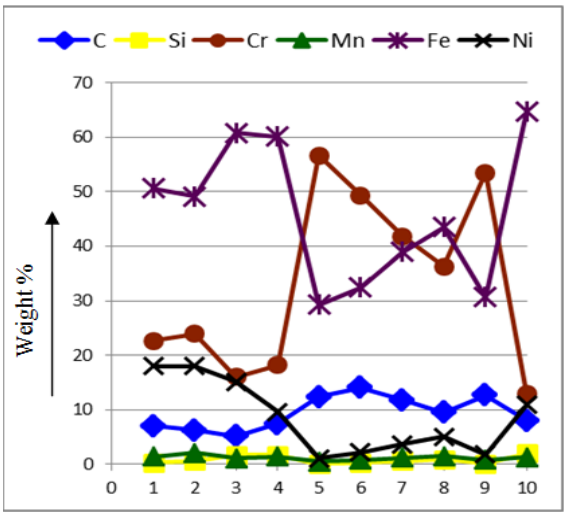

Fig. 3: Morphology and Elemental Composition at Different Points along the Cross-section of Hardfacing Overlay (HF)

of type M_7C_3 are discerned in the microstructure. These carbides are observed to be surrounded by eutectic of austenite-carbide matrix. The black region in the matrix is

eutectic austenite and the white region is the eutectic of carbides. The identified microstructural features have been ascertained through the review of similar structures reported in literature [30, 22, 31–35]. Identical to the observations reported in the literature, the micro-hardness at the hexagonal carbides is observed to be very high approaching to 1300Hv. The results of XRD and SEM-EDS analysis support the microstructural discussion of the hard face overlay. The microstructure seems to be highly refined after heat treatment (see Fig. 5(b)). The distribution of fine hexagonal carbides in the austenite-carbide matrix is highly uniform.

Micro-hardness

Table 4 shows the mean values of micro-hardness at different regions of cross-section and also on the surface. The hardness of the overlay is observed to be very high as compared to that of the base, which is believed to be due to the formation of carbides as indicated in microstructural and XRD analysis. The variation in micro-hardness can be observed at different points along the cross-section (see Fig. 6). Different microstructural phases may be the reason of this variation. The hardness of the heat treated overlay is observed to be high as compared to that of the base, which is due to the refinement of grain structure as inferred from Fig. 5(b).

Table 4: Average Micro-hardness at different Sections of Hardfacing

Hardface Overlay	Average Micro-hardness (Hv)		
	Base	Hardfacing	Surface
HF	246.24	555.01	565.81
HT	202.52	631.18	630.11

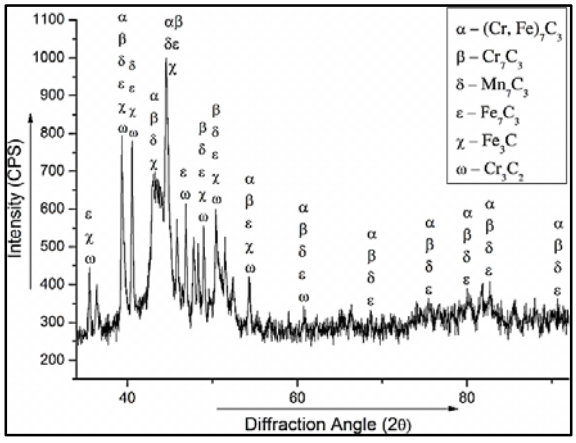

Fig. 4: XRD Analysis of Hardface Overlay HF

Erosion Performance and Effect of Heat Treatment

The weight loss suffered by each tested specimen is presented in the line chart in Fig. 7. Each reported value is the mean of weight loss suffered in three tests performed under similar conditions. In erosion testing of hardface overlays (with and without heat treatment), the weight loss is observed to be more in oblique impact erosion, tested at same temperatures. With the increase in temperature, the erosive weight loss increased in oblique impact testing, whereas decreased in normal impact testing. There was no change in the weight (or negligible change) of the additionally placed specimen in all high temperature tests. Therefore the erosion can be considered as pure metallic erosion without any effect of oxidation. Higher weight loss in oblique impact erosion as compared to that in normal impact, indicated the erosion occurred in ductile mode. Most of the metallic materials have been reported to be eroded in the ductile mode [36]. The efficient cutting mode due to deeper penetration of the erodent particles results in higher weight loss in oblique impact erosion.

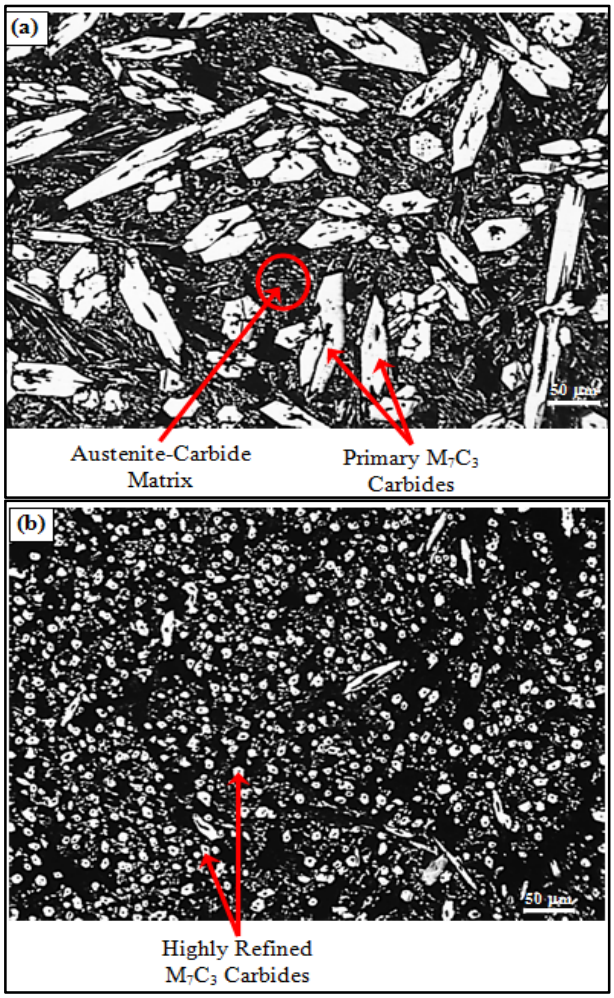

Fig. 5: Optical Micrographs Showing Surface Microstructure of Hardface Overlays (a) Before Heat Treatment (HF), (b) after Heat Treatment (HT)

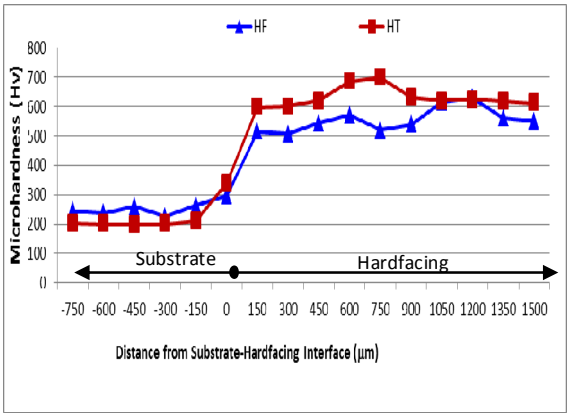

Fig. 6: Variation of Hardness Along the Cross-section of Hardfacing with and Without Heat-treatment

A significant improvement in the erosion resistance could be observed after heat treatment at both the angles of impingement. Highly refined grain structure of the heat treated overlay is believed to be the cause of this improvement (Fig. 5(b)). Grain refinement also resulted in the improvement in hardness but hardness is reported to have no direct relation with the erosion performance [37–39]. Uniform distribution of fine hexagonal hard carbides in the eutectic-carbide matrix is believed to have provided better erosion resistance after heat treatment. The softening of material occurs with the increase in temperature [40]. The normal force component of obliquely striking erodent particles enables the erodent particles penetrate deeper in the material softened at high temperature. Tangential component helps in longer travels of erodent particles in the material to remove large scoops of material resulting in higher material loss at elevated temperatures. In normal impact erosion testing, there is no tangential component of the force and the normal impacts extrude the material to oust the surrounding material. The lips thus created around the crater, are detached from the parent surface by the subsequent attacks of the erodent particles [36, 41]. After heat treatment, the highly refined grains microstructure restrains the plastic flow of material. It lowers the tendency of surrounding material to oust to create large lips, which separates from the parent metal by subsequent erodent impacts [40]. After heat treatment, the improvement in erosion resistance is observed to be more in oblique impact testing. The relationship between the hard carbides and soft matrix plays a decisive role in the erosion resistance of any two phase material. In case of oblique impact testing, it is believed that the ejection of coarse carbides result in higher weight loss. Whereas the carbides turned into very fine structure which improved its oblique impact erosion resistance significantly.

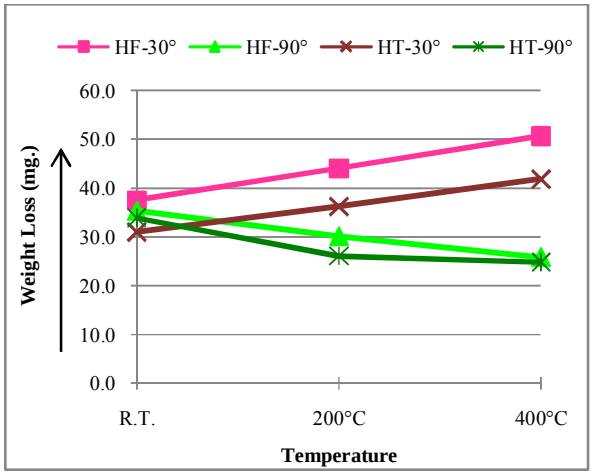

Fig. 7: Erosive Weight Loss at different Temperatures and Angles

CONCLUSION

The hardfacing electrode containing multiple carbide forming elements resulted in typical hypereutectic microstructure containing hard hexagonal carbides (of type M_7C_3) in relatively soft matrix of eutectic-carbide. Softening of material due to increase in temperature resulted in higher erosive weight loss under oblique impact erosion testing. Coarse hexagonal carbides transformed to very fine carbides after heat treatment. The uniform distribution of fine hexagonal carbides, bound strongly in carbide-eutectic matrix resulted in significant improvement in erosion resistance at all the test temperatures.

ACKNOWLEDGEMENT

The authors are grateful to Department of Science and Technology (DST), Govt. of India, New Delhi, India, for extending financial assistance to carry out this work through a research project entitled "Technological Innovations to Improve Degradation Resistance of Pulverized Coal Burner Nozzle (PCBN)".

REFERENCES

[1] Gat, N. and Tabakoff, W. (1978), "Some Effects of Temperature on the Erosion of Metals", *Wear*, Vol. 50, No. 1, pp. 85–94.

[2] Talia, M., Lankarani, H. and Talia, J.E. (1999), "New Experimental Technique for the Study and Analysis of Solid Particle Erosion Mechanisms, *Wear*, Vol. 225–229, Part 2, No. 0, pp. 1070–1077.

[3] Tu, J.P., Liu, M.S. and Mao, Z.Y. (1997), "Erosion Resistance of Ni-WC Self-fluxing Alloy Coating at High Temperature", *Wear*, Vol. 209, No. 1–2, pp. 43–48.

[4] ASTM-G40-13 (2013), "Standard Terminology Relating to Wear and Erosion", ASTM International, West Conshohocken, PA, Vol. 03.02, pp. 1–8.

[5] Mendez, P.F., Barnes, N., Bell, K., Borle, S.D., Gajapathi, S.S., Guest, S.D., Izadi, H., Gol, A.K., and Wood, G. (2014), "Welding Processes for Wear Resistant Overlays", *Journal of Manufacturing Processes*, Vol. 16, No. 1, pp. 4–25.

[6] Hidalgo, V.H., Varela, F.J.B., Menéndez, A.C. and Martínez, S.P. (2001), "A Comparative Study of High-temperature Erosion Wear of Plasma-sprayed NiCrBSiFe and WC–NiCrBSiFe Coatings under Simulated coal-fired Boiler Conditions", *Tribology International*, Vol. 34, No. 3, pp. 161–169.

[7] Stein, K.J., Schorr, B.S. and Marder, A.R. (1999), "Erosion of Thermal Spray MCr–Cr3C2 Cermet Coatings", *Wear*, Vol. 224, No. 1, pp. 153–159.

[8] Zhang, L., Sazonov, V., Kent, J., Dixon, T. and Novozhilov, V. (2001), "Analysis of Boiler-tube Erosion by the Technique of Acoustic Emission: Part I. Mechanical Erosion", *Wear*, Vol. 250, No. 1–12, pp. 762–769.

[9] Sidhu, B.S. and Prakash, S. (2006), "Erosion-corrosion of Plasma as Sprayed and Laser Remelted Stellite-6 Coatings in a Coal Fired Boiler", *Wear*, Vol. 260, No. 9–10, pp. 1035–1044.

[10] Yu, X.Q., Fan, M. and Sun, Y.S. (2002), "The erosion–corrosion behavior of Some Fe3Al-based Alloys at High Temperatures", *Wear*, Vol. 253, No. 5–6, pp. 604–609.

[11] Pekko, P. (2000), "Tetrahedral Amorphous Carbon Deposited with the Pulsed Plasma arc-discharge Method as a Protective Coating against solid Impingement Erosion", *Diamond and Related Materials*, Vol. 9, No. 8, pp. 1524–1528.

[12] Shanov, V. and Tabakoff, W. (1996), "Erosion Resistance of Coatings for Metal Protection at Elevated Temperatures", *Surface and Coatings Technology*, Vol. 86–87, Part 1, No. 0, pp. 88–93.

[13] Chatterjee, S. and Pal, T.K. (2006), "Solid particle Erosion behaviour of Hardfacing Deposits on Cast Iron—Influence of Deposit Microstructure and Erodent Particles", *Wear*, Vol. 261, No. 10, pp. 1069–1079.

[14] Katsich, C., Badisch, E., Roy, M., Heath, G.R. and Franek, F. (2009), "Erosive Wear of Hardfaced Fe–Cr–C Alloys at Elevated Temperature", *Wear*, Vol. 267, No. 11, pp. 1856–1864.

[15] Krishnamoorthy, P.R., Seetharamu, S. and Sampathkumaran, P. (1993), "Influence of the Mass Flux and Impact Angle of the Abrasive on the Erosion Resistance of Materials Used in Pulverized Fuel Bends and other Components in Thermal Power Stations", *Wear*, Vol. 165, No. 2, pp. 151–157.

[16] Hearley, J.A., Little, J.A. and Sturgeon, A.J. (1999), "The Erosion behaviour of NiAl Intermetallic Coatings Produced by High Velocity Oxy-fuel Thermal Spraying", *Wear*, Vol. 233–235, No. 0, pp. 328–333.

[17] Hoop, P.J. and Allen, C. (1999), "The High Temperature Erosion of Commercial Thermally Sprayed Metallic and Cermet Coatings by Solid Particles",*Wear*, Vol. 233–235, No. 0, pp. 334–341.

[18] Chandler, P.E. and Quigley, M.B.C. (1986), "The Application of Plasma Sprayed Coatings for the Protection of Boiler Tubing", in *Advances in Thermal Spraying*, W.I.O. Canada, Editor, 1986, Pergamon, pp. 29–35.

[19] Cutler, A.J.B., Flatley, T. and Hay, K. (1978), "Fire-side Corrosion in Power-station Boilers", *Central Electricity Research Labs*, Vol. 8, pp. 13–26.

[20] Hutchings, I.M. (1992), *Tribology: Friction and Wear of Engineering Materials*, 1992, CRC Press Taylor and Francis Group.

[21] Klimpel, A. and Kik, T. (2008), "Erosion and Abrasion Wear Resistance of GMA Wire Surfaced Nanostructural Deposits", *International Science Journal*, Vol. 30, No. 2, pp. 121–124.

[22] Sapate, S.G. and Rama Rao, A.V. (2004), "Effect of Carbide Volume Fraction on Erosive Wear behaviour of Hardfacing Cast Irons", *Wear*, Vol. 256, No. 7–8, pp. 774–786.

[23] Sapate, S.G. and Rama Rao, A.V. (2006), "Erosive Wear behaviour of Weld Hardfacing High Chromium Cast Irons: Effect of Erodent Particles", *Tribology International*, Vol. 39, No. 3, pp. 206–212.

[24] ASTM-A240/A240M-04a (2004), "Standard Specification for Chromium and Chromium-Nickel Stainless Steel Plate, Sheet, and Strip for Pressure Vessels and for General Applications", *ASTM International*, West Conshohocken, PA, pp. 1–12.

[25] Derringer, G. and Suich, R. (1980), "Simultaneous Optimization of Several Response Variables", *Journal of Quality Technology*, Vol. 12, No. 4, pp. 214–219.

[26] ASTM-G76-13 (2013), "Standard Test Method for Conducting Erosion Tests by Solid Particle Impingement Using Gas Jets", *ASTM International*, West Conshohocken, PA, Vol. 03.02, pp. 1–6.

[27] ASTM-E3-11 (2011), "Standard Guide for Preparation of Metallographic Specimens", *ASTM International*, West Conshohocken, PA, pp. 1–12.

[28] ASTM-B487-85 (2002), "Standard Test Method for Measurement of Metal and Oxide Coating Thickness by Microscopical Examination of a Cross Section", *ASTM International*, West Conshohocken, PA, pp. 1–5.

[29] ASTM-E384-99 (1999), "Standard Test Method for Microindentation Hardness of Materials", *ASTM International*, West Conshohocken, PA, pp. 1–24.

[30] Chen, J.-H., Hsieh, C.-C., Hua, P.-S., Chang, C.-M., Lin, C.-M., Wu, P.-Y. and Wu, W. (2013), "Microstructure and Abrasive Wear Properties of Fe-Cr-C Hardfacing alloy Cladding Manufactured by Gas Tungsten Arc Welding (GTAW)", *Metals and Materials International*, Vol. 19, No. 1, pp. 93–98.

[31] Chatterjee, S. and Pal, T.K. (2003), "Wear behaviour of Hardfacing Deposits on Cast Iron", *Wear*, Vol. 255, No. 1–6, pp. 417–425.

[32] Lu, L., Soda, H. and McLean, A. (2003), "Microstructure and Mechanical Properties of Fe–Cr–C Eutectic Composites", *Materials Science and Engineering: A*, Vol. 347, No. 1–2, pp. 214–222.

[33] Neville, A., Reza, F., Chiovelli, S. and Revega, T. (2006), "Characterization and Corrosion behavior of High-chromium White Cast Irons", *Metallurgical and Materials Transactions A*, Vol. 37, No. 8, pp. 2339–2347.

[34] Sabet, H., Mirdamadi, S., Kheirandish, S. and Goodarzi, M. (2013), "Effect of Volume Fraction of $(Cr,Fe)7C_3$ Carbides on Corrosion Resistance of the Fe-Cr-C Hardfacing Alloys at Cr/C=6", *Metalurgija -Journal of Metallurgy*, Vol. 19, No. 2, pp. 107–114.

[35] Dolman, K.F. (1983), "Alloy Develpment: Shredder Hammer Tips", in *Proc. of Australian Society of Sugar Cane Technologists*, Australia.

[36] Roy, M. (2006), "Elevated Temperature Erosive Wear of Metallic Materials", *J. Phys. D: Appl. Phys.*, Vol. 39, pp. R101–R124.

[37] Maiti, A.K., Mukhopadhyay, N. and Raman, R. (2007), "Effect of Adding WC Powder to the Feedstock of WC–Co–Cr Based HVOF Coating and its Impact on Erosion and Abrasion Resistance", *Surface and Coatings Technology*, Vol. 201, No. 18, pp. 7781–7788.

[38] Liu, S.-G., Wu, J.-M., Zhang, S.-C., Rong, S.-J. and Li, Z.-Z. (2007), "High Temperature Erosion properties of Arc-sprayed Coatings using Various Cored Wires Containing Ti–Al Intermetallics", *Wear*, Vol. 262, No. 5–6, pp. 555–561.

[39] Levy, A.V., Yan, J. and Patterson, J. (1986), "Elevated Temperature Erosion of Steels", *Wear*, Vol. 108, No. 1, pp. 43–60.

[40] Shimizu, K., Xinba, Y., Ishida, M. and Kato, T. (2011), "High Temperature Erosion Characteristics of Surface Treated SUS410 Stainless Steel", *Wear*, Vol. 271, No. 9–10, pp. 1349–1356.

[41] Hutchings, I.M. and Winter, R.E. (1974), "Particle Erosion of Ductile Metals: A Mechanism of Material Removal", *Wear*, Vol. 27, No. 1, pp. 121–128.